Spatially stochastic geometry and material properties in hygrothermal models

Michael Gutland[1], Scott Bucking[1], Mario Santana Quintero[1]
[1]Carleton University, Ottawa Ontario, Canada

Abstract

Performing hygrothermal simulations on historic wall assemblies presents a number of challenges. There are two often overlooked parameters when performing these analyses: (1) The effect's of decay has introduced many imperfections (cracks, mortar washout, failed membranes etc.) to the assembly; and (2) there is often a natural variance in the hygroscopic properties of historic building materials (and also repair materials) meaning that some units may be more absorptive or vapour permeable than others for example.

The positioning of materials with different properties are non-uniformally distributed throughout the wall. A spatially-stochastic approach to the building of geometry and assignment of material properties is proposed to be more suitable for this construction type. A series of hygrothermal models with stochastically assigned material properties was created given a known distribution of properties. The relative effect this had on simulation results was shown to be meaningful under drying, wetting and realistic boundary condition.

Introduction

Hygrothermal modelling of historic wall assemblies presents some unique challenges. Amongst these challenges are the unfamiliarity and poorer understanding of construction methods and materials compared to contemporary design; the inconsistency in material properties; and the effects of decay on the building fabric over time. The inability to grasp these factors complicates our ability to confidently model these types of assemblies whether assessing the U-value or the moisture response over the long-term. This has been hindered by difficulties calibrating hygrothermal models to in-situ measured data in terms of both heat and moisture transfer (Baker, 2011; Gutland, Santana Quintero, et al., 2019; Litti et al., 2015; Lucchi, 2017; Nardi et al., 2018). Calibration allows for the establishment of a dependable baseline model from which it is possible to confidently assess the assembly's current health, and project the positive and negative effects of retrofits on durability risk, energy performance and occupant comfort.

There are several possible reasons for calibration difficulties including the natural variability in material properties, uncertainty in the construction, composition and dimensions, simplifications in expressing geometry, and decay in the assembly. Part of the calibration problem can also be attributed to challenges of in-situ monitoring of masonry over an extended period (Agliata et al., 2018; Phillipson et al., 2007).

It is also proposed that the uncertainties in "seemingly random" geometry and material properties also contributes to calibration issues. When examining several of the historic stone walls in the Ottawa area, it can be seen that many walls have inconsistent geometry in the stone and mortar, inconsistent material and workmanship quality, and decay of material surfaces. These can be determined by visual inspection alone, but what lies unseen behind the surface can compound the problems with decay and defect mechanism such as the formation of voids. These factors are rarely considered in hygrothermal modelling where we assume simplified and homogeneous geometries, zero imperfections and deterministic material properties.

The topic of the "seemingly random" geometry was addressed in a previous paper (Gutland et al., 2022). Here a rubble-core sandstone wall was used as inspiration. This wall featured irregular sized stone units (height, width, depth), mortar and stone with dissimilar properties (thermal conductivity, liquid absorption, vapour diffusion) and known voids within the rubble core. The irregularly sized stones mean mortar joints can be more densely-packed in certain areas, and when combined with dissimilar material properties, leads to the formation of preferential heat and moisture paths. The air voids act like thermal insulators, capillary breaks and allow faster vapour diffusion and air circulation.

A Python script was written to stochastically create geometry of the rubble core walls based on an observed distribution of the geometry of the wythes and core stones, and the degree of voids. These detailed geometries were than simulated under four different sets of boundary conditions in Delphin 6.1 and compared with simplified 1-D series and 2-D parallel models.

The results of this project demonstrated that their was significant statistical variation in simulation results based and that simplified models were unable to adequately

replicate the more complicated geometries. That project forms the basis for the subsequent exploration of spatially-stochastic material properties. The idea for spatially-stochastic material properties comes from a collection of laboratory testing data for sandstone and mortar samples in the Ottawa region. The data for key hygrothermal properties (A_w, μ) have an uncomfortably high variance either side of the mean or median values. This is common for natural and historic manufactured materials where quality control could not be as guaranteed as it is with modern materials. This implies that depending on which end of the spectrum of properties is chosen in the simulation, a different story on the health and performance of the wall can be told, and both could be valid. A stochastic approach to material properties would therefore more appropriate.

Stochastic approaches to hygrothermal modelling are not new as first demonstrated by Salonvaara (2001). Further examples of stochastic hygrothermal models of masonry have been performed often with a view toward calibration (Akkurt et al., 2020; Freudenberg et al., 2017; Goffart et al., 2017; Gutland, Bucking, et al., 2019; Zhao et al., 2011).

While varying the material properties for each simulation, the conventional assumption is that all objects of the same class have the same material properties (ie. all bricks are the same), and any boundary conditions or air/water sources have no variation in the finite-element grid. As argued, this assumption is questionable on some occasions. It is hypothesized that the placement of these materials relative to one another is just as important of a factor. For example, a specific mortar material will behave differently when adjacent to a highly absorptive unit compared to a less absorptive unit, and behave differently when there is a good or bad contact between those surfaces (Interface Resistance, R_{IF}). This is something which would not be picked up in the traditional stochastic model.

This spatially-stochastic approach has been implemented in the structural analysis of historic masonry (Pulatsu et al., 2021). The mechanical properties of the units and mortar (e.g., compression strength), and the unit-mortar interfaces (e.g., stiffness, bond tensile strength, cohesion etc.) were assigned non-uniformally to each unit and joint in the discrete-element model. It was found that the spatially-stochastic models produced more consistent results with less scatter between the upper and lower bounds compared to non spatially-stochastic models.

In this paper, a methodology and rationale for spatially-stochastic material properties in a rubble-core masonry wall is outlined. Preliminary results are presented highlighting the variability in simulation results with discussion of what this means with regard to interpretation of results..Delphin 6.1 was used to perform the hygrothermal simulations (Bauklimatik Dresden, 2020)

Methods

The case study is a heritage-designated masonry building in Ottawa, Canada constructed between 1859-1867 and is in the process of being rehabilitated. It is known to have chronic moisture issues. The walls consist of sandstone inner and outer wythes sandwiching a rubble core consisting of smaller stones, grouted with a poured mortar. The stones, mortar joints and core stones are of different sizes. Combined with numerous wall thicknesses, pilasters water-shedding courses and ornamentation, it is challenging to define a clear-field assembly.

Geometry

The stack pattern used and the general nature of rubble core construction give the building a seemingly random geometry which is difficult to generalize. Stones of different sizes (height, width, thickness) are used in the construction of the wythes. With the aid of rectified photogrammetric images, the sizes of the wythe stones, mortar joints and core stones were estimated and a normal distribution of their dimensions determined. Using this distribution, a Python script was written to stochastically create 500 mm tall by 600 mm thick wall sections that could be translated into Delphin's XML input format. The result is a set of unique model geometries representative of the many cross-sections of the real building (Figure 1).

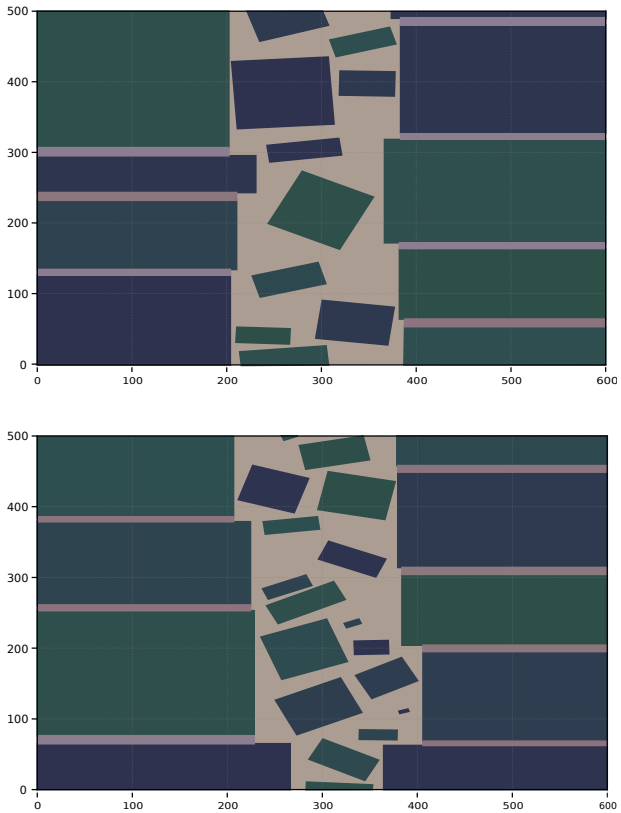

Figure 1: examples of rubble core geometry showing the varying dimensions of stones and core thicknesses.

A detailed description of how the geometry of the models was created can be found here (Gutland et al., 2022). Each stone and mortar joint would than be assigned a unique material file (as the different colours in the image show). Voids in the rubble core were not considered in this study.

Material Properties

The primary type of stone used in the clear-field walls is Nepean Sandstone which is very dense and has a low porosity for a sandstone. It tends to have low absorption and higher vapour resistance. Other types of sandstone are used around window arches, quoin stones and water-shedding courses which are not included in this study.

The original mortar (joints and grouted core) would have been lime based. Samples of this original mortar tend to have higher porosity and are more absorptive. The original mortars have been steadily decaying over time and maintenance including re-pointing, bedding mortar replacement and even re-grouting has been undertaken. The replacement mortars have been of varying formulations (including Portland – based and Roman cement) and quality compared to the original mortars. Decay has been a persistent issue as visually evident by open mortar joints, friable mortars and also unseen pathologies such as binder washout in the core.

Laboratory testing has been conducted on the Nepean Sandstone and mortars in different batches and by different laboratories. Data was collected from the various public and private sources and a statistical analysis was performed on the key hygrothermal property data. Most mortar samples were not labelled as what their mix composition were. They could be representative of 100+ year old mixes or replacement mortars. Some mortar samples were denoted as having coatings which changed their vapour transport properties. These data points were omitted.

Another complicating factor was that some of the laboratories used different measurement methods. Most of the vapour diffusion tests were performed under wet-cup conditions. These are not as accurate as dry-cup measurement for input into Delphin where vapour transport ($k_v(\theta_l)$) and liquid transport ($k_l(\theta_l)$) are modelled distinctly (wet-cup measurements include a degree of capillary transport). The wet-cup measurements were converted into an estimated dry-cup vapour permeability using Equation 1:

$$k_{v,dry} = \frac{k_{v,wet}}{\chi} \quad (1)$$

Here the variable χ is a scaling variable to signify the difference between the two measurement methods. A comparison of one set of data points were high as a factor of 6.0. A study of historic stones and masonry in Scotland showed on average that χ would be equal to 2.0 for both a range of sandstones and heritage mortars (Banfill, 2020). This value was chosen to convert the wet-cup measurements. This likely moved the vapour resistance factor (μ) of sandstone lower compared to some dry-cup measurements which were quite high ($\mu > 100$).

Testing data was sparse for thermal conductivity and heat capacity. Stochastic values were obtained using a normal distribution with the mean and standard deviation estimated from previous calibration models and materials from the Delphin library.

Data for the moisture retention curves and moisture-dependant liquid conductivity curves were not available. They were obtained by modifying the Delphin library materials Sandstone Oberkirchner and Red Lime Plaster. These materials most closely matched the known porosity, pore distribution and absorption characteristics of the Nepean sandstone and mortar.

Upon analysing, it was recognized that many important properties had large standard deviation and skewness. The statistical distributions for stone and mortar are given in Table 1. Skewness was significant for some properties, especially the absorption coefficient (A_w) which were weighted toward the lower end of the scale. 32 unique material files were created where the properties in each file

Table 1: Statistical distribution of material properties

	Nepean Sandstone			Mortar		
	Mean	Standard Deviation	Skewness	Mean	Standard Deviation	Skewness
λ_{dry} [W/m-K]	2.5	0.56	0	0.9	0.18	0
C_p [J/kg-K]	850	60	0	950	150	0
θ_{eff} [--]	0.086	0.037	-0.380	0.221	0.049	0.119
ρ [kg/m^3]	2370.9	111.8	0.420	1935.0	119.3	-1.367
A_w [kg/m^2-$\sqrt{s}$]	0.0171	0.0138	0.969	0.0446	0.0261	1.341
$k_{v,dry}$ [s]	5.395 E-12	2.880 E-12	0.117	4.930 E-12	2.541 E-12	1.0761
μ_{dry} [--]*	36.1	--	--	39.5	--	--

* Calculated fom $k_{v,dry}$

were randomly selected from the skew normal distributions with calculated mean, standard deviation and skewness. Each stone rectangle and mortar joint was randomly assigned one of these unique material files.

Around each stone–mortar interface an interface resistance (R_{IF}) was assigned. From site observations it is known that there are joints with hairline fractures and larger gaps. This will inhibit moisture transport between stone and mortar and joints than those with much better contacts. Based on this observation, the interface resistances were randomly assigned assuming a log normal distribution because it is not feasible to measure this from samples. Here each interface has a value of 10^x m/s where x is taken from a Gaussian distribution with mean 10 and standard deviation of 2.

Boundary Conditions

The spatially-stochastic models were simulated under different boundary conditions:

1. **Steady-state heat transfer** – Imposed surface temperatures of T_{out} = 1°C and T_{in} = 0°C (no surface convection or radiation). Moisture transport not modelled. Duration = 120 h to establish equilibrium.
2. **Drying** – Initial RH = 99%, RH_{out} = RH_{in} = 50%. Heat transport not modelled. Duration = 120 days to allow for measurable drying in the core.
3. **Wetting** – Initial RH = 50%, Pulsed rain load of 1 kg/m^{2}h on exterior face for 8 hours every day for a duration of 90 days to guarantee adequate penetration of the moisture front past the outer wythe. Heat transport not modelled.
4. **Actual Weather Years** – 2 years of real weather data from the Ottawa International Airport (*Environment and Climate Change Canada*, 2020; Saha et al., 2011)

Standard heat and moisture convection coefficients were used. Interior conditions were modelled according to ASHRAE 160's simplified method (ASHRAE, 2009). For Boundary Condition 4, the wind-driven rain exposure was assumed to have an F_EF_D of 1.0 indicating relatively high moisture loadings.

Simulation Procedure

A number of simulations were performed using Delphin to explore the effect of spatially-stochastic material properties. 16 unique geometries were created each with 32 unique iterations with random assignment of material properties and interface resistances. These geometries could conceivably be stitched together to form one long wall section. Using multiple geometry sets improves the odds of the many geometric characteristics of these type of wall (eg. dense or loosely spaced mortar joints, stone heavy rubble cores) to be reflected in the statistical analysis.

Each combination was simulated under each of the four boundary conditions. The relevant state variables (T, RH, Q_{heat}, Q_{water}) were recorded at pre-determined wall depths at regular time intervals.

Results and Discussion

Steady-State Heat Transfer

The results of the steady-state heat transfer simulations are shown in the violin plots of Figure 2. A violin shows the mean and relative spread for each geometry modelled. For heat transfer, the mean values are consistent between geometries varying from 3.09 to 3.29 W/m^2. Some geometries seemed to produce tighter variances (Geometry

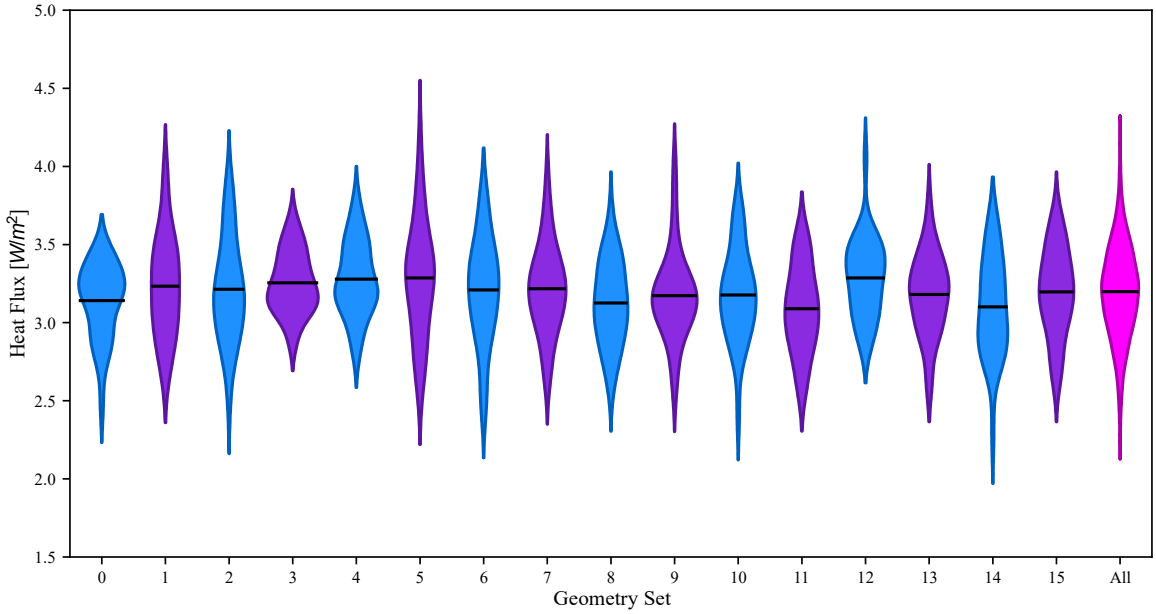

Figure 2: Distributions of steady-state heat flux simulations

3, σ = 0.193 W/m^2) and some produce looser variances (Geometry 5, σ = 0.362 W/m^2).

In the previous project where the material properties were deterministic, there was a strong correlation observed between the ratio of stone/mortar in a solid wall and the recorded heat flux. That broke down considerably with spatially-stochastic material properties (Figure 3). Previously the correlation of determination for this was r^2=0.885, and that has been reduced to r^2=0.465.

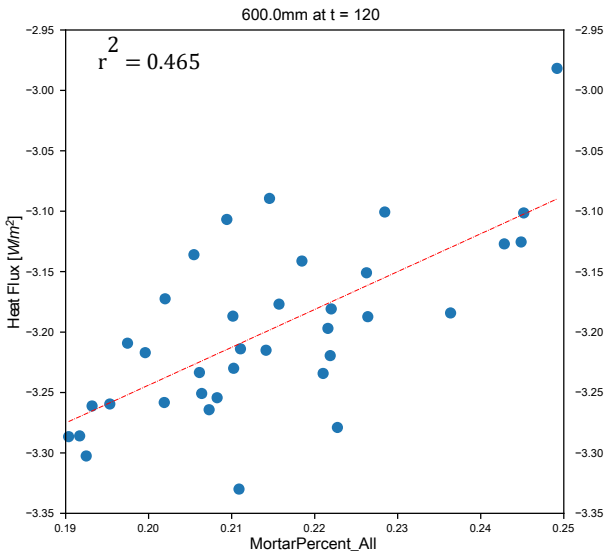

Figure 3: Scatter plot of mean heat flux and mortar ratio of full cross-section of wall.

Drying

The results of the drying simulations are shown in the violin plots of Figure 4 which show the amount of moisture lost. There is a variation in the mean of geometry sets between 2.70 and 3.40 kg/m^3. There was a modest correlation between the percentage of mortar in each geometry set and the moisture lost (r^2=0.42) which can partially explain this variation in means. A few extreme data points were observed with the lowest total moisture loss of 1.68 kg/m^3 and maximum of 4.44 kg/m^3 (45% and 46% below the mean value observed. This max/min range was reflected in the moisture flux data too.

A significant variation in the drying front could be observed from the RH data. At a line 100 mm into the wall, a difference of up to 13.8% in mean RH could be found between different simulations performed with the same geometry set. RH at this depth range from a minimum of 79.0% to 98.0% across all simulations and geometry sets, however the results skewed towards the wetter end of the scale. Other geometry sets only showed a difference of 6%. This demonstrates that across a long wall section there will be an uneven drying front with observable pockets of dry and damp because of the natural variation in material properties.

Wetting

The results of the wetting simulations are shown in the violin plots of Figure 5. There isn't a large relative variation between the means of each geometry set in terms of moisture absorbed, with geometry 8 being an exception. On average 16.0 kg/m^3 of water are absorbed with an average standard deviation of 2.76 kg/m^3. This represents a four to five-fold increase in moisture content (initial conditions vary depending on material combinations). The maximum observed increase was 24.8 kg/m^3 and the

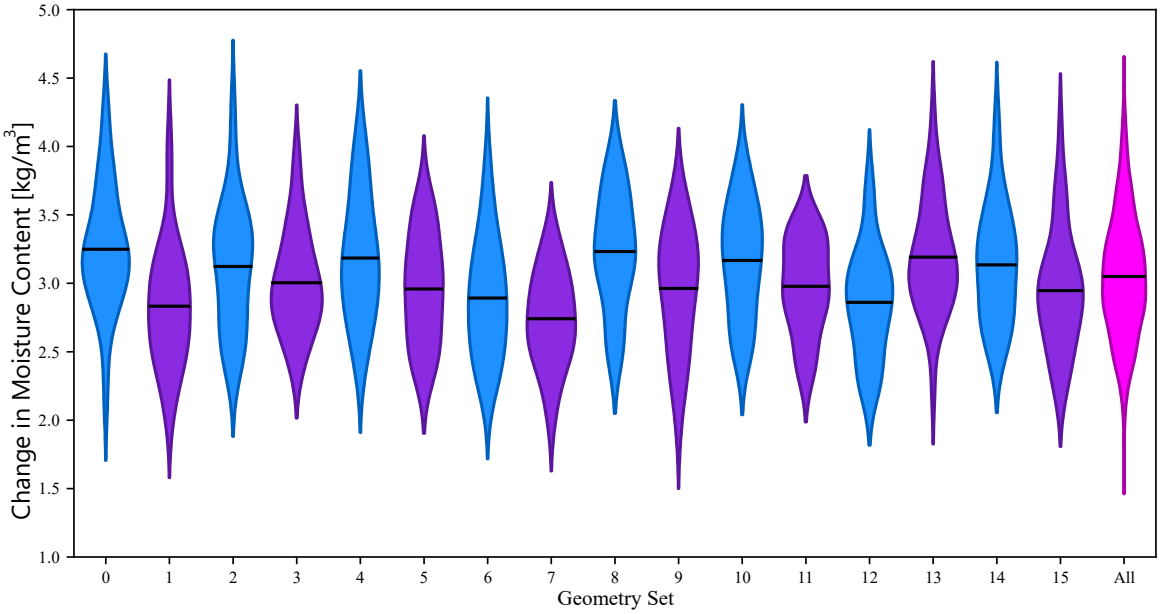

Figure 4: Distributions of the simulated change in Moisture Content under drying conditions

minimum increase was 6.70 kg/m^3. The relative max/min ranges relative to the mean are comparable to those found in the drying simulations (58% and 53% respectively).

In the previous project where the material properties were deterministic, there was a robust correlation between the stone/mortar ratio and both the amount of moisture gained and the moisture flux ($r^2 > 0.99$). With spatially-stochastic material properties this strong correlation broke down significantly ($r^2 = 0.20$ for moisture gained and r^2 0.37 for moisture flux at the outer wythe.). In fact there was a stronger correlation between the ratio of stone/mortar in the core. This was unanticipated and is attributable to changes in porosity and the amount of moisture gained under the extreme wetting conditions simulated. Whereas liquid conductivity appeared to be the dominant material property with deterministic material properties, porosity appears to play a more significant role with spatially-stochastic properties.

Actual Weather Year

For the actual weather year simulations, there was significant variation between simulations of the same geometry set in terms of moisture accumulation. Typically the mean value was approximately 4.0 kg/m^3 gained from the beginning of the simulation. There were a few examples which absorbed almost twice this amount, and some which absorbed very little over the duration of the simulation.

In terms of relative humidity significant variation can be found throughout the simulated year. Figure 6 shows the mean, and 2σ quantile ranges for the relative humidity at 2/3 depth into the wall for all simulations over the final year. While the mean RH is still relatively high, there is a long tail of much drier simulation results (range >15% at some timesteps). The skew towards high RH may be a result of the high moisture loadings applied to the wall and the nature of the moisture content curve. Small changes at elevated RH equate to a larger increase in moisture content than at lower RH. It is expected the skew will even out if moisture loadings are reduced. Similar conclusions can be drawn when broken down for each geometry set.

In terms of net annual heat flux, there was a much tighter variance compared to moisture statistics. There was only a maximum ±18% range from the mean which was comparable to the steady-state simulations. The 2σ quantile ranges for instantaneous heat flux are shown in Figure 7. A similar skewed distribution can be found in the heat flux time series as RH (and moisture flux too). An interesting note is that each of these variables skews to higher RH, and that more favourable outcomes do occur, but are less likely.

The results were also analysed using damage indices like RHT, critical RH and number of freeze thaw cycles. The RHT Index is calculated as follows:

$$RHT = \Sigma(RH_{avg} - 80) * (T_{avg} - 5) \quad if \;\; RH_{avg} > 80 \text{ and } T_{avg} > 5 \tag{2}$$

In terms of RHT, there wasn't a large difference in values detected in the outer 2/3 of the wall. This is likely because this part of the wall is consistently wet throughout the year (RH > 95). The inner third is where significant variation begins to be observed and is of special concern if trying to judge the durability risk of embedded components such as joist ends or lintels. If using the monthly mean RH and T for the RHT Index, a skewed distribution is observed with a mean value of approximately 2000 while approximately

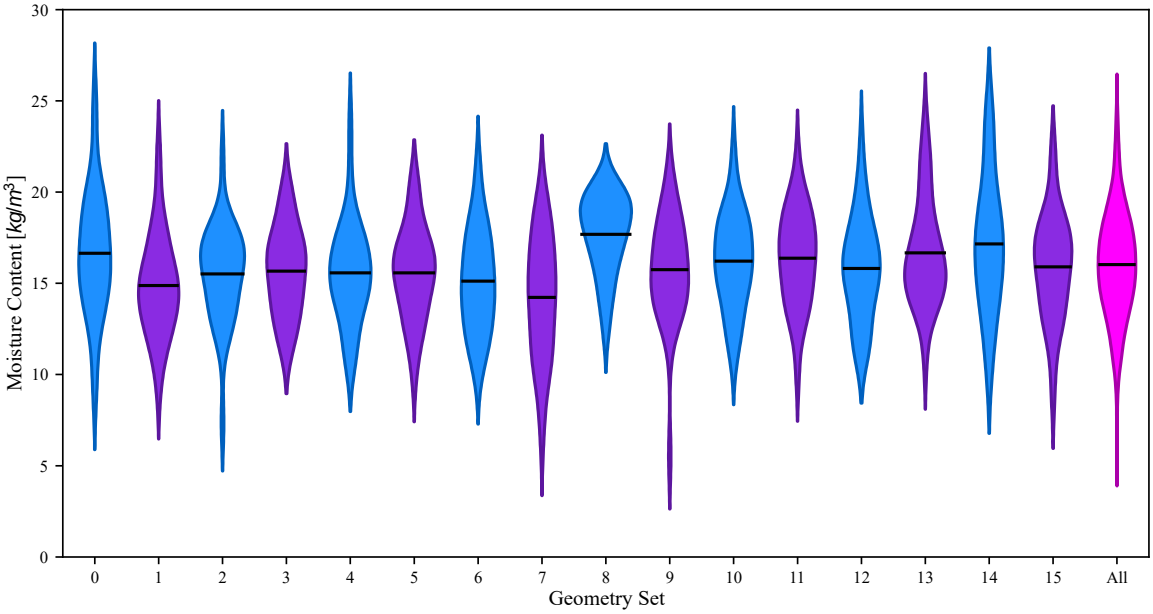

Figure 5: Distributions of the simulated change in Moisture Content under drying conditions

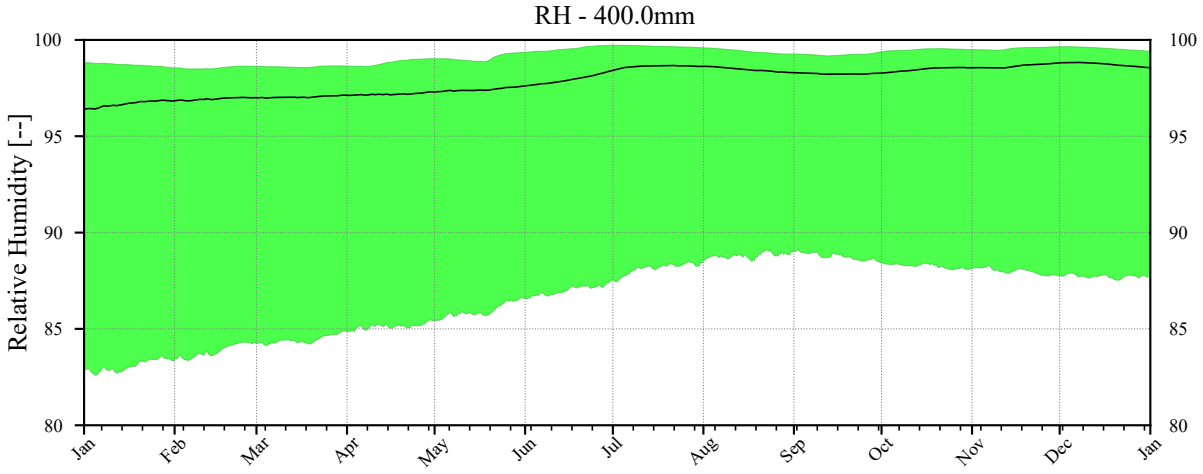

Figure 6: 2σ quantile range for RH on the final year of simulation

15% of simulations have less than 1000. This is indicative of a combination of materials which either have an outer wythe which is low absorbing or an inner wythe which has low vapour resistance.

The number of freeze thaw cycles observed did not vary significantly between simulations. There was some variation in the number of critical freeze-thaw cycles (assuming critical degrees of saturation of both 50% and 75%) especially in the mortar. This was consistent with expectations and is likely related to changes in porosity of the mortar.

Conclusion

The results of the spatially-stochastic simulations demonstrate a significant statistical variance largely independent of geometry sets used. This was observed under all four boundary conditions used. Under several performance metrics, a statistical skew was observed which tended to be weighted towards the higher (and more unfavourable) end of the scale. More favourable outcomes like lower RH, heat flux do occur, but are less likely.

The next steps in this project are to compare the results of the spatially-stochastic runs to the more traditional stochastic approach. It is expected that this spatially-stochastic approach will produce less statistical variance, fewer extreme results and require fewer simulations to achieve a statistical interpretation of the results..

This approach can be applied to other wall types. Material testing of Ottawa area heritage brick shows similar variance in its material properties to that of the Nepean and heritage mortar. Double and triple wythe brick construction could be created taking a similar approach of stochastic geometry (to a lesser degree than rubble core masonry) and spatially-stochastic properties. This approach could also be used in the absence of material property testing data by using randomly selecting materials from the WUFI or Delphin libraries.

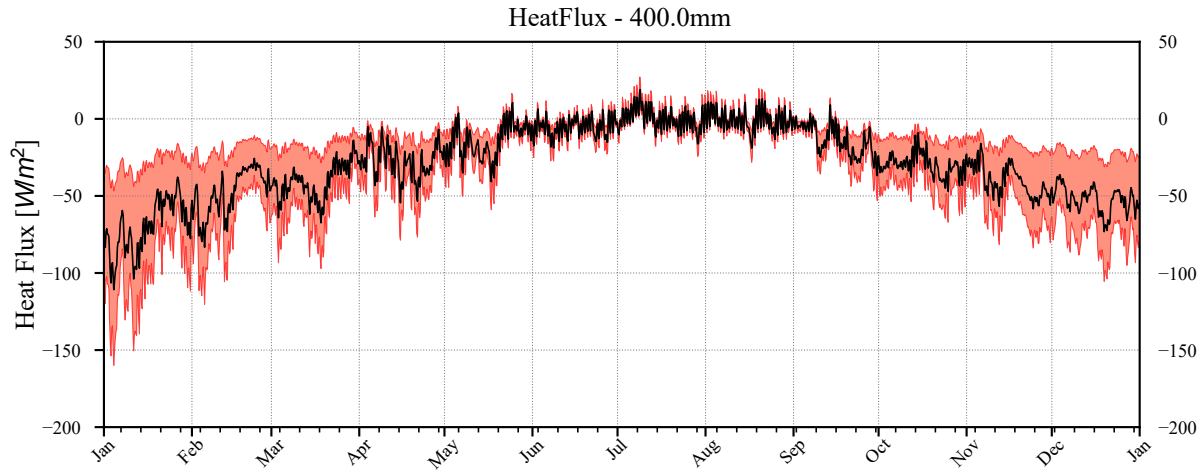

Figure 7: 2σ quantile range for heat flux on the final year of simulation. Negative values equal flow to the outside

References

Agliata, R., Mollo, L., & Greco, R. (2018). Moisture measurements in heritage masonries: A review of current methods. Materials Evaluation, 76, 1468–1477.

Akkurt, G. G., Aste, N., Borderon, J., Buda, A., Calzolari, M., Chung, D., Costanzo, V., Del Pero, C., Evola, G., Huerto-Cardenas, H. E., Leonforte, F., Lo Faro, A., Lucchi, E., Marletta, L., Nocera, F., Pracchi, V., & Turhan, C. (2020). Dynamic thermal and hygrometric simulation of historical buildings: Critical factors and possible solutions. Renewable and Sustainable Energy Reviews, 118, 109509. https://doi.org/10.1016/j.rser.2019.109509

ASHRAE. (2009). ASHRAE Standard 160-2009, Criteria for Moisture-Control Design Analysis in Buildings. American Society of Heating, Refrigerating and Air-Conditioning Engineers.

Baker, P. (2011). U-values and traditional buildings—In situ measurements and their comparisons to calculated values (Technical Paper 10). Historic Scotland.

Banfill, P. F. (2020). Hygrothermal properties of Scottish building stone and mortar. Proceedings of BSO-V 2020, 6.

Bauklimatik Dresden. (2020). *DELPHIN 6.1* (6.1.0) [Computer software]. https://bauklimatik-dresden.de/delphin/index.php?aLa=en

Freudenberg, P., Ruisinger, U., & Stöcker, E. (2017). Calibration of Hygrothermal Simulations by the Help of a Generic Optimization Tool. Energy Procedia, 132, 405–410. https://doi.org/10.1016/j.egypro.2017.09.645

Goffart, J., Rabouille, M., & Mendes, N. (2017). Uncertainty and sensitivity analysis applied to hygrothermal simulation of a brick building in a hot and humid climate. Journal of Building Performance Simulation, 10(1), 37–57. https://doi.org/10.1080/19401493.2015.1112430

Gutland, M., Bucking, S., & Santana Quintero, M. (2019). Assessing Durability of Historic Masonry Walls with Calibrated Energy Models and Hygrothermal Modeling. International Journal of Architectural Heritage, 1–17. https://doi.org/10.1080/15583058.2019.1618976

Gutland, M., Bucking, S., & Santana Quintero, M. (2022). Hygrothermal modelling of historic rubble masonry walls: Accounting for geometric and compositional variability. Journal of Building Engineering, 48, 103929. https://doi.org/10.1016/j.jobe.2021.103929

Gutland, M., Santana Quintero, M., & Bucking, S. (2019, September). Calibration of an historic masonry building using measured temperature and heat flux data. Proceedings of Building Simulation 2019: 16th Conference of IBPSA. Building Simulation 2019, Rome, Italy.

Historical Data. (2020). Environment and Climate Change Canada. http://climate.weather.gc.ca/historical_data/search_historic_data_e.html

Litti, G., Khoshdel, S., Audenaert, A., & Braet, J. (2015). Hygrothermal performance evaluation of traditional brick masonry in historic buildings. Energy and Buildings, 105, 393–411. https://doi.org/10.1016/j.enbuild.2015.07.049

Lucchi, E. (2017). Thermal transmittance of historical stone masonries: A comparison among standard, calculated and measured data. Energy and Buildings, 151, 393–405. https://doi.org/10.1016/j.enbuild.2017.07.002

Nardi, I., Lucchi, E., de Rubeis, T., & Ambrosini, D. (2018). Quantification of heat energy losses through the building envelope: A state-of-the-art analysis with critical and comprehensive review on infrared thermography. Building and Environment, 146, 190–205. https://doi.org/10.1016/j.buildenv.2018.09.050

Phillipson, M. C., Baker, P. H., Davies, M., Ye, Z., McNaughtan, A., Galbraith, G. H., & McLean, R. C. (2007). Moisture measurement in building materials: An overview of current methods and new approaches. Building Services Engineering Research and Technology, 28(4), 303–316. https://doi.org/10.1177/0143624407084184

Pulatsu, B., Gonen, S., Erdogmus, E., Lourenço, P. B., Lemos, J. V., & Prakash, R. (2021). In-plane structural performance of dry-joint stone masonry Walls: A spatial and non-spatial stochastic discontinuum analysis. Engineering Structures, 242, 112620. https://doi.org/10.1016/j.engstruct.2021.112620

Saha, S., Moorthi, S., Wu, X., Wang, J., Nadiga, S., Tripp, P., Behringer, D., Hou, Y.-T., Chuang, H., Iredell, M., Ek, M., Meng, J., Yang, R., Mendez, M. P., van den Dool, H., Zhang, Q., Wang, W., Chen, M., & Becker, E. (2011). NCEP Climate Forecast System Version 2 (CFSv2) Selected Hourly Time-Series Products. Research Data Archive at the National Center for Atmospheric Research, Computational and Information Systems Laboratory. https://doi.org/10.5065/D6N877VB

Salonvaara, M., Karagiozis, A., & Holm, A. (2001). Stochastic Building Envelope Modeling—The Influence of Material Properties. Buildings VIII Proceedings, 8.

Zhao, J., Plagge, R., Nicolai, A., Grunewald, J., & Zhang, J. S. (2011). Stochastic study of hygrothermal performance of a wall assembly—The influence of material properties and boundary coefficients. HVAC&R Research, 17(4), 591–601. https://doi.org/10.1080/10789669.2011.585421